A R C H I V E O F M E C H A N I C A L E N G I N E E R I N G

VOL. LXII 2015 Number 1

10.1515/meceng-2015-0007

Key words: finite element method, vibration analysis, experimental verification

IWONA ADAMIEC-WÓJCIK [*], *ANDRZEJ NOWAK* [**], *STANISŁAW WOJCIECH* [***]

MODELLING PLATES AND SHELLS BY MEANS OF THE RIGID FINITE ELEMENT METHOD

The rigid finite element method (RFEM) has been used mainly for modelling systems with beam-like links. This paper deals with modelling of a single set of electrodes consisting of an upper beam with electrodes, which are shells with complicated shapes, and an anvil beam. Discretisation of the whole system, both the beams and the electrodes, is carried out by means of the rigid finite element method. The results of calculations concerned with free vibrations of the plates are compared with those obtained from a commercial package of the finite element method (FEM), while forced vibrations of the set of electrodes are compared with those obtained by means of the hybrid finite element method (HFEM) and experimental measurements obtained on a special test stand.

1. Introduction

The process of dust removal from the collecting electrodes significantly influences the effectiveness of the electrostatic precipitators. The maximal values of tangent and normal accelerations occurring during the work of precipitators are important parameters used in their evaluation. For engineers, it is also important that the accelerations are evenly distributed over the surface of the electrode. The accelerations depend both on the geometry of the system (thickness, length and shape) and the force inducing the vibrations. Fig. 1 presents a single section of the collecting electrodes which is modelled and analysed.

[*] *University of Bielsko-Biała, ul. Willowa 2, 43-309 Bielsko-Biała, Poland; E-mail: i.adamiec@ath.eu*

[**] *University of Bielsko-Biała, ul. Willowa 2, 43-309 Bielsko-Biała, Poland; E-mail: a.nowak@ath.eu*

[***] *University of Bielsko-Biała, ul. Willowa 2, 43-309 Bielsko-Biała, Poland; E-mail: swojciech@ath.eu*

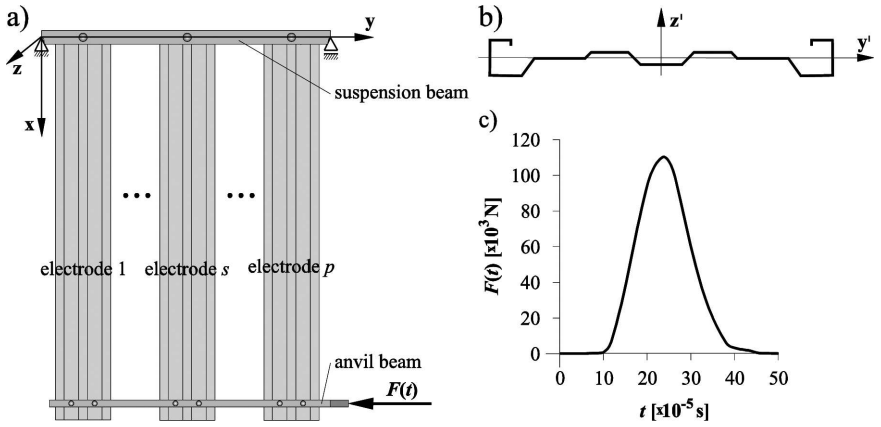

Fig. 1. A single set of the collecting electrodes: a) general view, b) shape of the electrode SIGMA VI, c) typical course of the impact force

The authors have already dealt with the problem of modelling of this system [1-4]. Two methods, the hybrid finite element method (HFEM) [5, 6] and finite element method (FEM), have been used up to now for modelling the electrodes [7]. However, the upper and bottom beams are discretized using the RFEM [8]. Beams and electrodes are connected by means of spring--damping elements [4]. In this paper the classical RFEM is used for modelling the whole system: the beams and the electrodes. The hybrid finite element method [3] used the RFEM for discretisation, but the energy of spring deformation of the collecting electrodes was calculated by means of the classical finite element method. A special element with 24 node values was defined and the flexible coordinates (deformations in nodes) were expressed by means of the coordinates of rigid finite elements. In the approach presented here, the spring-damping features of shells are expressed by spring-damping elements.

The stiffness coefficients for plates defined in [5] (with some modifications described in the next sections) are used. Computer implementation enables us to compare the results of calculations with those obtained by the hybrid finite element method and by experimental measurements.

2. REFM – Primary Division

A characteristic feature of the RFEM is the two-step division of the system discretised: primary and secondary division. In the case of the electrodes the primary division can be carried out in accordance with the strips and then into rectangular areas (Fig. 2).

If we assume that the electrode has m strips with length L and width b_j ($j = 1, \ldots, m$) and that each strip can be divided into n rectangles with sides

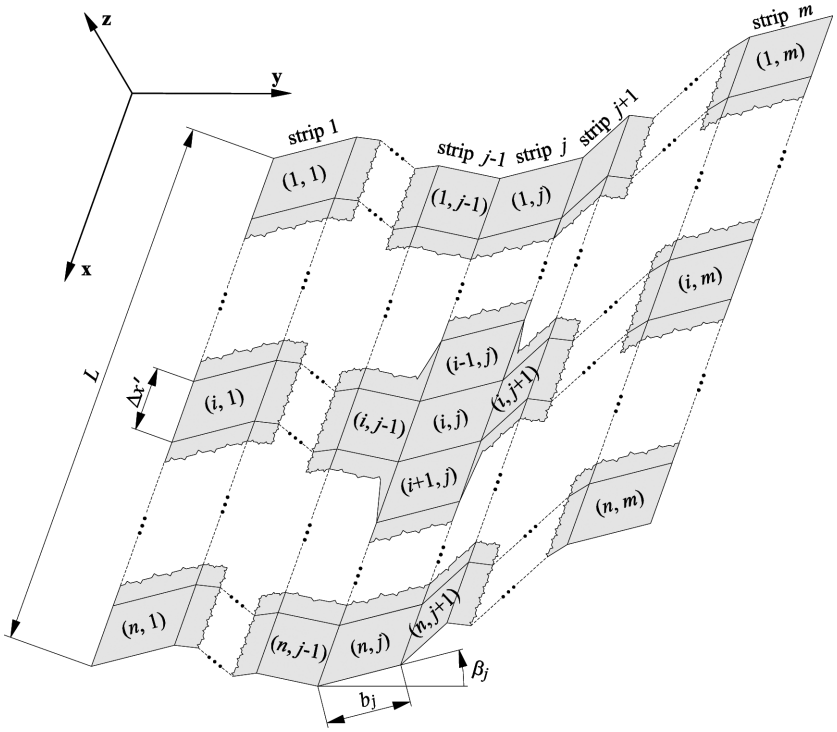

Fig. 2. Division of the electrode with m strips into primary elements

b_j and $\Delta x'$:

$$\Delta x' = \frac{L}{n}. \tag{1}$$

The number of the elements in the primary division is equal to:

$$N_p = n \cdot m. \tag{2}$$

The next stage in the RFEM is to replace elastic features of the elements obtained as a result of the primary division by spring-damping elements (sde). In the classical approach [5], elastic features are represented by means of sdes placed as in Fig. 3a. Segments 1 to 4 into which the elements are divided have five degrees of freedom:

u', v', z' – translational displacements,

$\varphi_{x'}, \varphi_{y'}$ – rotational displacements,

and stiffness coefficients are defined by the following relations:

$$\left.\begin{aligned} c_{12}^{x'} = c_{34}^{x'} &= \frac{Eh\Delta y'}{2\Delta x'} & c_{23}^{x'} = c_{41}^{x'} &= \frac{Gh\Delta x'}{2\Delta y'} \\ c_{12}^{y'} = c_{34}^{y'} &= \frac{Gh\Delta y'}{2\Delta x'} & c_{23}^{y'} = c_{41}^{y'} &= \frac{Eh\Delta x'}{2\Delta y'} \\ c_{12}^{z'} = c_{34}^{z'} &= \frac{Gh\Delta y'}{2\Delta x'} & c_{23}^{z'} = c_{41}^{z'} &= \frac{Gh\Delta x'}{2\Delta y'} \\ c_{12}^{\varphi_{x'}} = c_{34}^{\varphi_{x'}} &= \frac{Gh^3\Delta y'}{12\Delta x'} & c_{23}^{\varphi_{x'}} = c_{41}^{\varphi_{x'}} &= \frac{Eh^3\Delta x'}{24\left(1-\nu^2\right)\Delta y'} \\ c_{12}^{\varphi_{y'}} = c_{34}^{\varphi_{y'}} &= \frac{Eh^3\Delta y'}{24\left(1-\nu^2\right)\Delta x'} & c_{23}^{\varphi_{y'}} = c_{41}^{\varphi_{y'}} &= \frac{Gh^3\Delta x'}{12\Delta y'} \end{aligned}\right\}, \qquad (3)$$

where E is the Young's modulus, G is the shear modulus, ν is the Poisson number, h is the thickness of the electrode. A characteristic feature of this classical approach is the possibility of rotation of segments 1 to 4 about the axes perpendicular to the surface of the primary element. Thus, rotation about this axis for the four corner elements of the plate is not blocked. However, for the electrodes (shells) with a complicated shape it is necessary to assume that the motion of the segment is described by six degrees of freedom (three translational and three rotational displacements). Paper [9] presents an approach in which the sdes are shifted to positions as in Fig. 3b. For the analysis in this paper, the positions of sdes are assumed to be as in Fig. 3c [10]. This eliminates the singularities connected with lack of limitations of rotary motion about $\mathbf{z}'$ axis of corner elements, which are characteristic of the classical approach. In the case presented in Fig. 3b torsional vibrations are also eliminated.

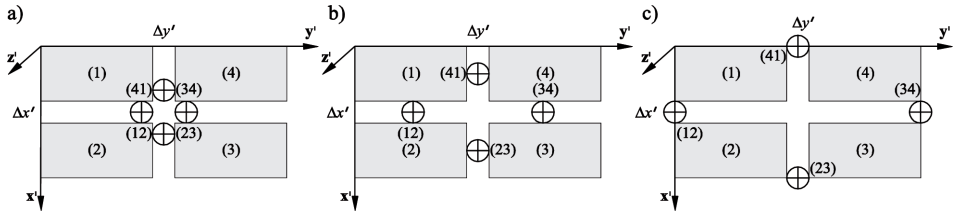

Fig. 3. Position of sdes(⊕) in the primary element: a) classical RFEM [5] b) proposed by [9] c) proposed in this paper

3. RFEM – Secondary Division

The secondary division consists in connecting neighbouring segments (one, two or four) belonging to different primary elements into rigid finite

elements (rfe) as shown in Figs 4 and 5a. As a result the electrode is divided into:

$$N_w = (m+1)(n+1) \tag{4}$$

rigid elements (rfe). A system of main inertial axes $\left\{\mathbf{x}'_{C,k}, \mathbf{y}'_{C,k}, \mathbf{z}'_{C,k}\right\}$ of the element is assigned to rfe k. Axis $\mathbf{x}'_{C,k}$ is parallel to axis $\mathbf{x}$ of base coordinate system {}. Axis $\mathbf{y}'_{C,k}$ is inclined to the reference coordinate system, making angle α_k with axis $\mathbf{y}$ (Fig. 5b).

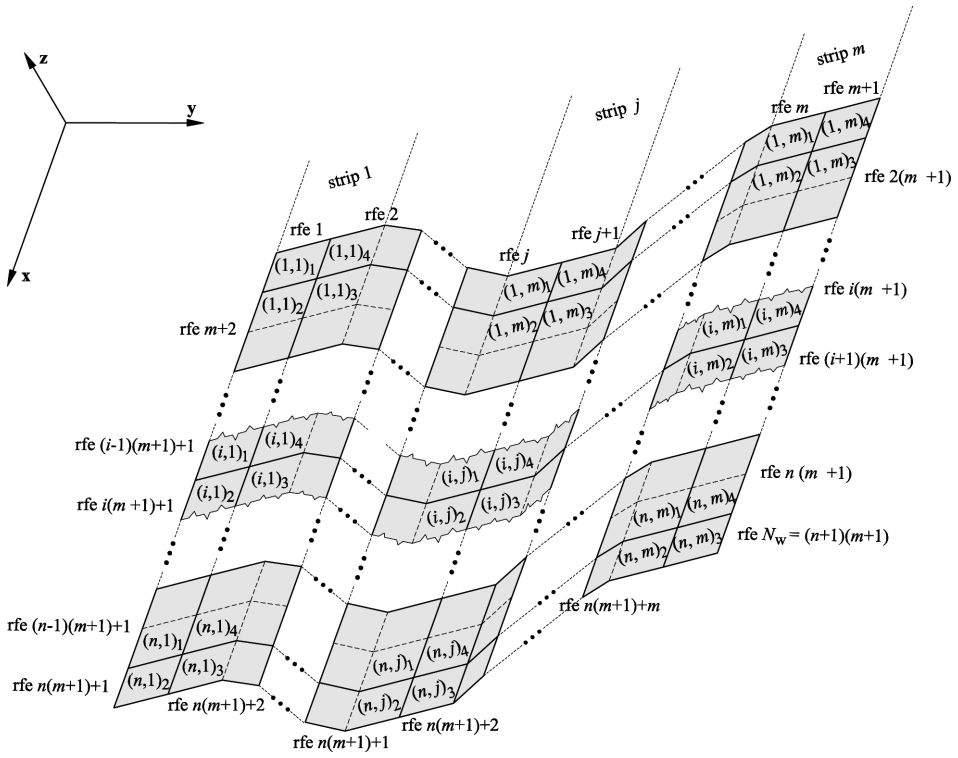

Fig. 4. Numbering of rigid elements of electrode s

The generalized coordinates of rfe k are the elements of the vector:

$$\mathbf{q}'_k = \left[x'_k, y'_k, z'_k, \varphi'_{x,k}, \varphi'_{y,k}, \varphi'_{z,k}\right]^{\mathrm{T}}, \tag{5}$$

where x'_k, y'_k, z'_k are translational displacements, $\varphi'_{x,k}, \varphi'_{y,k}, \varphi'_{z,k}$ are rotational displacements.

Displacements which are the components of the above vector are defined with respect to the undeformed state of the system. The vector of the generalized coordinates of electrode s takes the form:

$$\mathbf{q}'^{(s)} = \left[\mathbf{q}'^{(s)\mathrm{T}}_1 \ldots \mathbf{q}'^{(s)\mathrm{T}}_k \ldots \mathbf{q}'^{(s)\mathrm{T}}_{N_w}\right]^{\mathrm{T}} \tag{6}$$

and its kinetic energy can be written as follows:

$$T^{(s)} = \frac{1}{2}\dot{\mathbf{q}}'^{(s)\mathrm{T}}\mathbf{M}^{(s)}\dot{\mathbf{q}}'^{(s)}, \tag{7}$$

where $\mathbf{M}^{(s)}$=diag$\left\{ \mathbf{M}_1^{(s)} \ \ldots \ \mathbf{M}_k^{(s)} \ \ldots \ \mathbf{M}_{N_w}^{(s)} \right\}$ is a matrix with constant elements; $\mathbf{M}_k = \mathrm{diag}\left\{m_k, m_k, m_k, I_{x,k}, I_{y,k}, I_{z,k}\right\}$; m_k is the mass of element k; $I_{x,k}, I_{y,k}, I_{z,k}$ are mass inertial moments of rfe k with respect to axes of coordinate system $\left\{\mathbf{x}'_{C,k}, \mathbf{y}'_{C,k}, \mathbf{z}'_{C,k}\right\}$. Quantities $\alpha_k, m_k, I_{x,k}, I_{y,k}, I_{z,k}$ can be easily calculated in an algorithmic way [1-4].

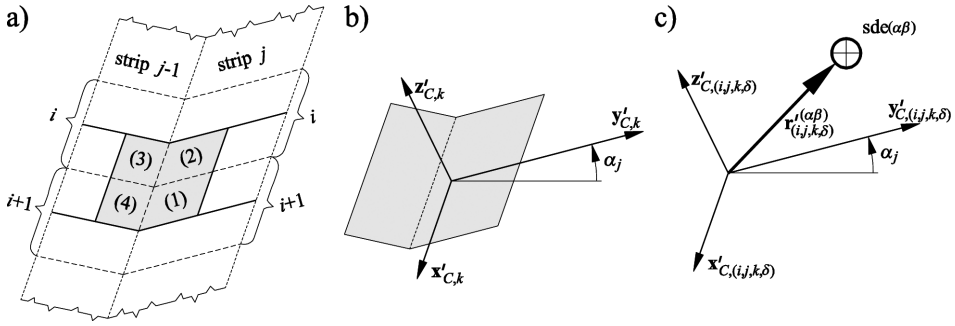

Fig. 5. Rfe k: a) connection of segments of different primary elements, b) main central axes of inertia, c) denotation of coordinates of an sde in the local coordinate system of a rfe

4. Energy of deformation of SDE

It is assumed that (s, i, j, δ) is the number of rfes which contain segment δ of primary element (i, j) of electrode s. The potential energy of the spring deformation of the electrode can be written in the following form:

$$V^{(s)} = \sum_{i=1}^{m}\sum_{j=1}^{n} V_{i,j}^{(s)}, \tag{8}$$

where $V_{i,j}^{(s)}$ is the energy of deformation of the sde of primary element (i, j) of electrode s. Values $V_{i,j}^{(s)}$ have to be dependent on the generalized coordinates of rfes $(s, i, j, 1)$ to $(s, i, j, 4)$. In view of Fig. 3b it is assumed that:

$$\begin{aligned} V_{i,j}^{(s)} = {} & \frac{1}{2}\Delta_{s,i,j,12}^{\mathrm{T}}\mathbf{C}_{s,i,j,12}\Delta_{s,i,j,12} + \frac{1}{2}\Delta_{s,i,j,23}^{\mathrm{T}}\mathbf{C}_{s,i,j,23}\Delta_{s,i,j,23} + \\ & + \frac{1}{2}\Delta_{s,i,j,34}^{\mathrm{T}}\mathbf{C}_{s,i,j,34}\Delta_{s,i,j,34} + \frac{1}{2}\Delta_{s,i,j,41}^{\mathrm{T}}\mathbf{C}_{s,i,j,41}\Delta_{s,i,j,41} \end{aligned}, \tag{9}$$

where $\mathbf{C}_{s,i,j,12}, \mathbf{C}_{s,i,j,23}, \mathbf{C}_{s,i,j,34}, \mathbf{C}_{s,i,j,41}$ are diagonal 5×5 matrices with elements defined by (3), having assumed the parameters of element (i, j) of electrode s; $\Delta_{s,i,j,12}, \Delta_{s,i,j,23}, \Delta_{s,i,j,34}, \Delta_{s,i,j,41}$ are deformations of sdes. Deformations of sdes are expressed in the coordinate systems of primary element (i, j), which is inclined towards axis $\mathbf{y}$ of the inertial system at angle β_j. Since axes $\mathbf{y}'_{C,k}$ are inclined towards axis $\mathbf{y}$ at angle α_j, having assumed denotations as in Fig. 5c, coordinates of sde $(s, i, j, \alpha\beta)$ with respect to the coordinate system of rfes (s, i, j, α) and (s, i, j, β) can be defined according to the formulae:

$$\mathbf{r}'^{(C,\alpha\beta)}_{(s,i,j,\alpha)} = \mathbf{U}^{(\alpha\beta)}_{(s,i,j,\alpha)} \mathbf{q}'_{(s,i,j,\alpha)} + \mathbf{r}'^{(\alpha\beta)}_{(s,i,j,\alpha)}, \tag{10.1}$$

$$\mathbf{r}'^{(C,\alpha\beta)}_{(s,i,j,\beta)} = \mathbf{U}^{(\alpha\beta)}_{(s,i,j,\beta)} \mathbf{q}'_{(s,i,j,\beta)} + \mathbf{r}'^{(\alpha\beta)}_{(s,i,j,\beta)}, \tag{10.2}$$

where

$$\mathbf{U}^{(\alpha\beta)}_{(s,i,j,\delta)} = \begin{bmatrix} 1 & 0 & 0 & 0 & z'_{(s,i,j,\delta)} & -y'_{(s,i,j,\delta)} \\ 0 & 1 & 0 & -z'_{(s,i,j,\delta)} & 0 & x'_{(s,i,j,\delta)} \\ 0 & 0 & 1 & y'_{(s,i,j,\delta)} & -x'_{(s,i,j,\delta)} & 0 \end{bmatrix}, \quad \mathbf{r}'^{(\alpha\beta)}_{(s,i,j,\delta)} = \begin{bmatrix} x'^{(\alpha\beta)}_{(s,i,j,\delta)} \\ y'^{(\alpha\beta)}_{(s,i,j,\delta)} \\ z'^{(\alpha\beta)}_{(s,i,j,\delta)} \end{bmatrix}$$

is the vector of local coordinates of sde $\alpha\beta$ in coordinate system $\left\{\mathbf{x}'_{C,(s,i,j,\delta)}, \mathbf{y}'_{C,(s,i,j,\delta)}, \mathbf{z}'_{C,(s,i,j,\delta)}\right\}$, $\delta = 1, 2$.

Coordinates (10) can be expressed with respect to the system of element (i, j) using the formulae:

$$\mathbf{r}'_{(s,i,j,\alpha)} = \mathbf{R}^{\mathrm{T}}_{(s,i,j)} \mathbf{R}_{(s,i,j,\alpha)} \mathbf{r}'^{(C,\alpha\beta)}_{(s,i,j,\alpha)}, \tag{11.1}$$

$$\mathbf{r}'_{(s,i,j,\beta)} = \mathbf{R}^{\mathrm{T}}_{(s,i,j)} \mathbf{R}_{(s,i,j,\beta)} \mathbf{r}'^{(C,\alpha\beta)}_{(s,i,j,\beta)}, \tag{11.2}$$

where $\mathbf{R}_{(s,i,j)}$, $\mathbf{R}_{(s,i,j,\delta)}$ are transformation matrices with constant elements [4].

Expression from (9) in the following form:

$$V^{(s,\alpha\beta)}_{i,j} = \tfrac{1}{2} \Delta^{\mathrm{T}}_{s,i,j,\alpha\beta} \mathbf{C}_{s,i,j,\alpha\beta} \Delta_{s,i,j,\alpha\beta}, \tag{12}$$

means that the equations of motion contain 6×6 sub-matrices of the stiffness matrix due to differentiating the spring energy (12) with respect to $\mathbf{q}'_{(s,i,j,\alpha)}$ and $\mathbf{q}'_{(s,i,j,\beta)}$.

5. Synthesis of Equations, model Validation

The approach used in this work consists in the direct use of formulae for stiffness coefficients for plate elements given in [5], with some modification.

Computer implementation of this approach enables us to compare calculation results with those obtained using the software package Abaqus based on the finite element method. The analysis is concerned with free vibrations of plates. For the set of electrodes the results are compared with those obtained by means of the hybrid finite element method and experimental measurements.

5.1. Synthesis of the equations

Discretisation of the upper and bottom beams as well as the method of connecting the beams with electrodes and the impact force $F(t)$ from Fig. 1c are described in detail in previous papers [1,2]. Having used the relation presented in sections 3 and 4, the equations of motion can be presented in the following form:

$$\mathbf{M}\ddot{\mathbf{q}} + \mathbf{C}\mathbf{q} = \mathbf{G} + \mathbf{Q}, \tag{13}$$

where $\mathbf{M}$ is the diagonal mass matrix; $\mathbf{C}$ is a the stiffness matrix; $\mathbf{G}$ is the vector of gravity forces; $\mathbf{Q}$ is the vector of generalised forces induced by the impact; $\mathbf{q} = \left[\begin{array}{ccccccc} \mathbf{q}'^{(g)\mathrm{T}} & \mathbf{q}'^{(1)\mathrm{T}} & \dots & \mathbf{q}'^{(s)\mathrm{T}} & \dots & \mathbf{q}'^{(p)\mathrm{T}} & \mathbf{q}'^{(d)\mathrm{T}} \end{array} \right]^{\mathrm{T}}$, $\mathbf{q}'^{(s)}$ defined in (7), $\mathbf{q}'^{(g)}$, $\mathbf{q}'^{(d)}$ are vectors of generalised coordinates of the beams. When the upper and bottom beams are divided into $n^{(g)}$ and $n^{(d)}$ rigid elements respectively, then the number of elements of vector $\mathbf{q}$ equals:

$$N = 6\left[n^{(g)} + \sum_{s=1}^{p} N_w^{(s)} + n^{(d)}\right], \tag{14}$$

where $N_w^{(s)} = \left(n^{(s)} + 1\right)\left(m^{(s)} + 1\right)$. Matrices $\mathbf{M}$ and $\mathbf{C}$ and vector $\mathbf{G}$ have constant elements.

The Newmark method is used in order to integrate equations (13). Since matrix $\mathbf{M}$ is diagonal and matrix $\mathbf{C}$ is sparse, special numerical procedures for solving algebraic sparse linear systems are used.

5.2. Results of numerical calculations

Verification of the model presented is carried out by analysing free vibrations of a single unbounded plate. Results obtained are compared with results from ABAQUS. Frequencies of free vibrations are calculated by solving the problem:

$$\det(\mathbf{I} - \omega^2\mathbf{M}^{-1}\mathbf{C}) = 0. \tag{15}$$

In order to choose the appropriate density of discretisation, several test calculations of frequencies of free vibrations of the flat rectangular steel plate with dimensions 1 m × 4 m and thickness 0.0015 m were carried out. The parameters of the plate are as follows: density ρ = 7850 kg/m^3, Young modulus $E = 2.06 \cdot 10^{11}$ Pa, Poisson number ν = 0.3. The first 50 frequencies of free vibrations are compared. We assume that the density of discretisation is reliable if the maximal difference between the values of frequencies obtained from two consecutive discretisation steps is smaller than 2%. The optimal size of discrete elements for RFEM and ABAQUS (ABQ) used for verification and validation of the model are defined on the basis of the chart presented in Fig. 6. For further analysis the following rectangular elements are assumed: 0.1 m × 0.2 m for the authors' model, 0.05 m × 0.05 m for ABAQUS. The thickness is 0.0015 m, which is typical for the collecting electrode. Moreover, the model in ABAQUS uses a standard shell element with default physical and numerical parameters.

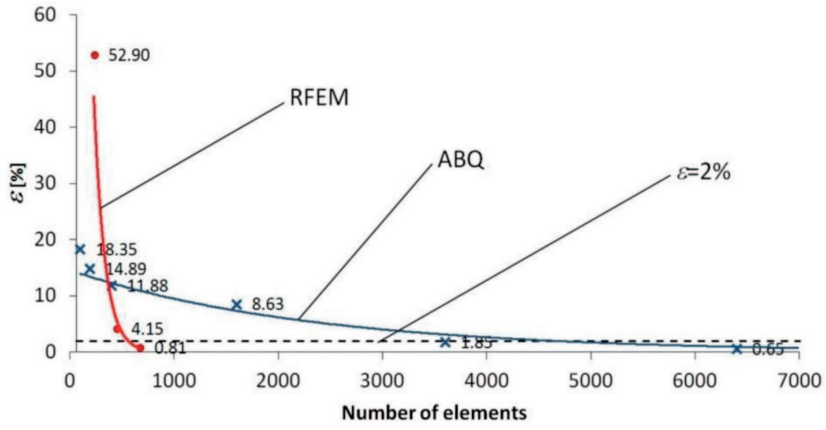

Fig. 6. Identification of the optimal density of discretization

Fig. 7a shows a comparison of the first 50 frequencies of free vibrations of the steel plate with dimensions 0.5 m × 16 m and thickness 0.0015 m. These dimensions reflect the longest collecting electrodes used in industrial electrostatic precipitators. Denotations used are as follows: RFEM – results obtained by the authors' model, ABQ – results obtained by ABAQUS.

It is important to note that the differences between the values of frequencies of free vibrations obtained with the model described and the commercial software are smaller than 5% (Fig. 7b). Such results have also been obtained for the model in which the number of discrete elements is a quarter of that used in the commercial software; this allows significantly shorter calculation times.

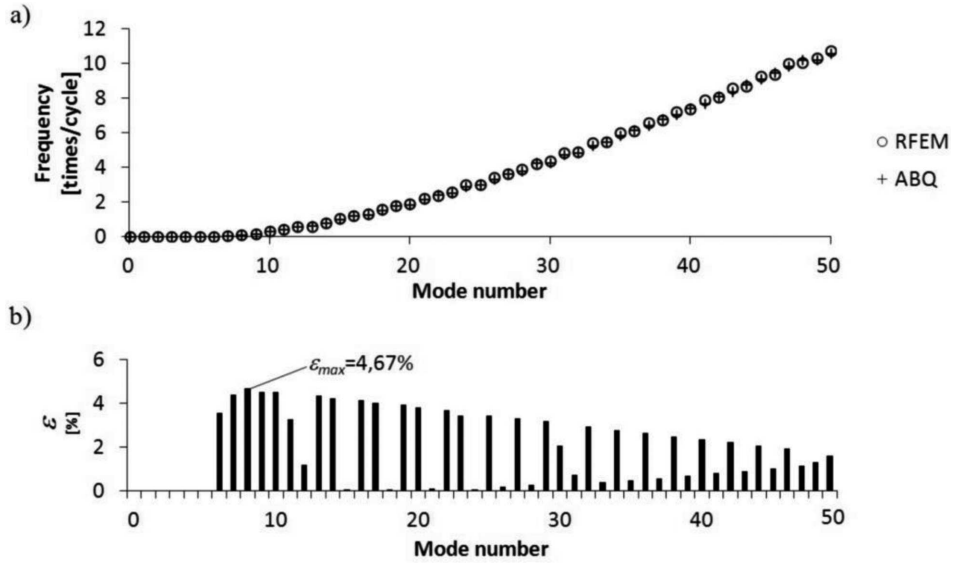

Fig. 7. Free vibrations of the plate: a) first 50 frequencies of free vibrations, b) relative differences in values of frequencies

5.3. Model validation

The model is validated by comparison of the results of calculations with experimental measurements carried out on a special test stand [4]. A computer programme in Delphi 7.0 was developed on the basis of the model presented. Vibrations of the system analysed can be simulated for different geometrical and mass parameters, for example different number, length and thickness of the electrodes or different number of strips in the electrode. Different dimensions of the beams and different courses of the impulse force can be also analysed.

The results of calculations for the system of electrodes were compared with those measured on the test stand (Fig. 8a). The impulse force is presented in Fig. 1c. The test stand contains nine SIGMA VI collecting steel electrodes which are 16.152 meters long and 0.0015 m thick.

In order to eliminate vibrations resulting from other sources than the beater, its drive was switched off. The motion of the beater started by being released from the position shown in Fig. 8b and finished by hitting the anvil (Fig. 8c). The measurements were carried out in calm conditions, temperature about 20 degrees centigrade, using the apparatus consisting of: three–axial vibration sensors ICP 356A02 made by PCB Piezotronics, recorder TEAC LX110 and a laptop with LX Navi software. Signals were registered at a frequency of 24 kHz for each channel. Sensors were glued to the surface of

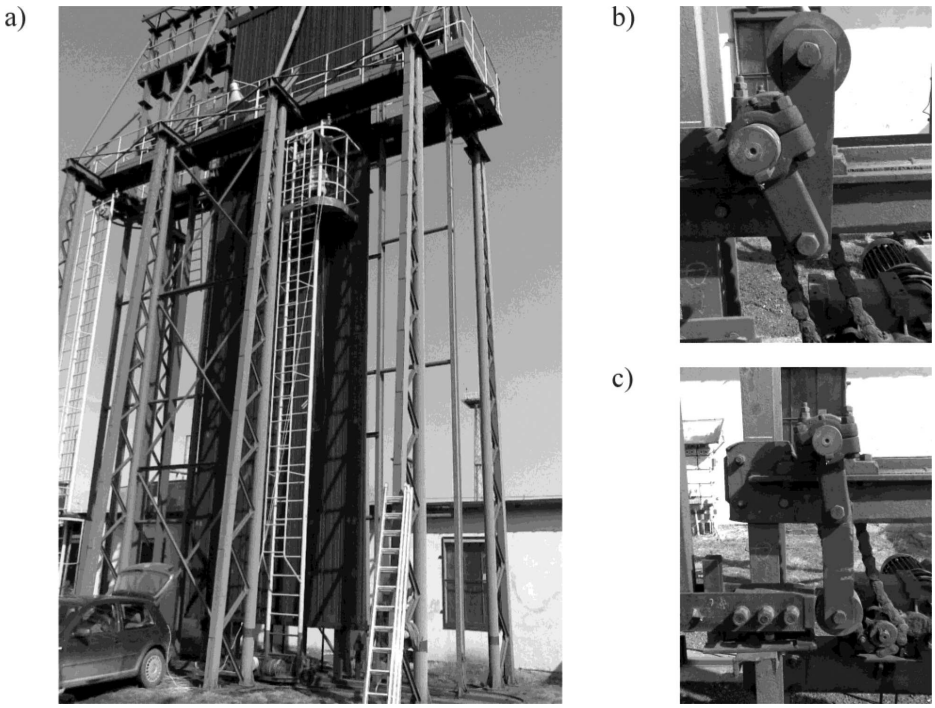

Fig. 8. Test stand: a) general view, b) initial and c) final position of the beater

the collecting electrodes. The scheme of position of the measurement points is presented in Fig. 9.

Vibrations of the electrodes are fast alternating processes and the direct comparison of courses is not effective. Thus for the comparative analysis two coefficients are used, $FAC2$ and q_ε, defined as follows:

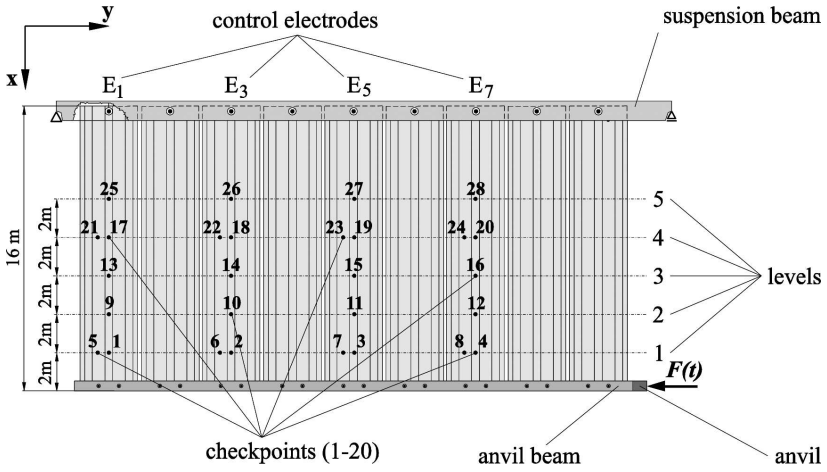

Fig. 9. Configuration of the control points in the system

$$FAC2\,(a_s) = \frac{1}{n_p}\sum_{i=1}^{n_p} N_i^f, \tag{16.1}$$

$$q_\varepsilon\,(a_s) = \frac{1}{n_p}\sum_{i=1}^{n_p} N_i^q, \tag{16.2}$$

where

$$N_i^f = \begin{cases} 1 & \text{for } \frac{1}{2} \le \dfrac{W^o\left(a_s^{(i)}\right)}{W^p\left(a_s^{(i)}\right)} \le 2 \\ 0 & \text{otherwise} \end{cases}, N_i^q = \begin{cases} 1 & \text{for } \dfrac{\left|W^o\left(a_s^{(i)}\right)\right| - \left|W^p\left(a_s^{(i)}\right)\right|}{\left|W^p\left(a_s^{(i)}\right)\right|} \le \varepsilon, \\ 0 & \text{otherwise} \end{cases}$$

i is the number of the control point, n_p is the number of control points, $W^\gamma = \max_{0\le t\le T}|a_s|$, $T$is the calculation time, $\gamma \in \{o,\ p\}, W^o\left(a_s^{(i)}\right)$ are values obtained from the calculations, $W^p\left(a_\alpha^{(i)}\right)$ are values of the experimental measurements, $s = (\nu, \tau, c)$ denotes normal, tangent and overall acceleration respectively. Results are considered to be acceptable when the coefficients $FAC2\,(a_s) \ge 0.5$ and $q_\varepsilon\,(a_s) \ge 0.66$ for the examined value $\varepsilon = 0.4$. Both coefficients are presented in Fig. 10.

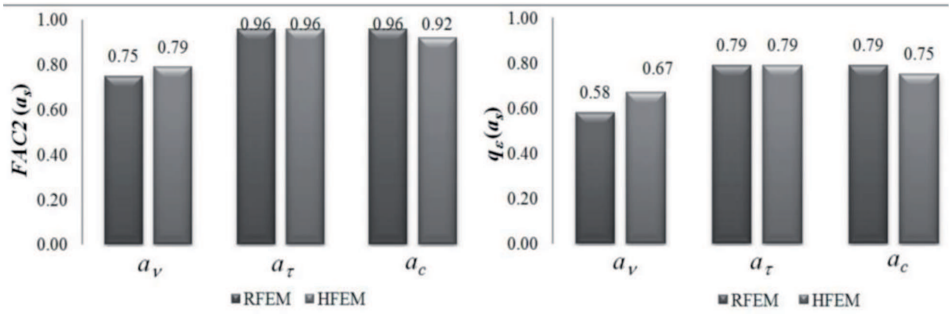

Fig. 10. Validation: coefficients $FAC2_\gamma\,(a_s)$ and $q_\gamma\,(a_s)$ for $s = (\nu, \tau, c)$

Calculations based on the authors' model were carried out with an integration step of 5×10^{-6} s. Time of analysis is 0.02 s.

6. Conclusions

In the approach proposed in this paper, we use formulae for stiffness coefficients for plate elements defined in the classical formulation of the RFEM. However, the position of sdes resulting from the primary division is modified. The new approach is used for analysis of a simple unbounded rectangular plate and for a system of plates with complicated shapes which are collecting

electrodes. Frequencies of free vibrations are compared with those obtained by commercial software, while dynamic vibrations of the collecting plates are compared with results obtained from the hybrid method and experimental measurements. Good compatibility of results has been achieved. The RFEM enables us to formulate a model of a system with shell elements with a relatively small number of degrees of freedom, which increases numerical effectiveness of calculations.

Manuscript received by Editorial Board, October 12, 2014;
final version, February 08, 2015.

REFERENCES

[1] Adamiec-Wójcik I., Nowak A., Wojciech S.: Comparison of methods for vibration analysis of electrostatic precipitators. Acta Mech. Sinica, 1 (Vol. 27), 2011, pp. 72-79.

[2] Adamiec-Wójcik I.: Modelling of Systems of Collecting Electrodes of Electrostatic Precipitators by means of the Rigid Finite Element Method, Archive of Mechanical Engineering. Volume 58, Issue 1, pp. 27-47, DOI: 10.2478/v10180-011-0002-x

[3] Adamiec-Wójcik I., Awrejcewicz J., Nowak A., Wojciech S.: Vibration Analysis of Collecting Electrodes by means of the Hybrid Finite Element Method, Mathematical Problems in Engineering, Volume 2014, Article ID 832918, 19 pages, 2014. doi:10.1155/2014/832918.

[4] Nowak A: Modelling and measurements of vibrations of collecting electrodes of dry electrostatic precipitators, (in Polish: Modelowanie i pomiary drgań elektrod osadczych elektrofiltrów suchych). Bielsko-Biała, Rozprawy Naukowe 35, Wydawnictwo Naukowe Akademii Techniczno-Humanistycznej, Bielsko-Biała, 2011.

[5] Kruszewski J., Gawroński W., Wittbrodt E., Najbar F., Grabowski S.: Metoda sztywnych elementów skończonych,(in Polish: The Rigid Finite Element Method). Arkady, Warszawa, 1975.

[6] Gawroński W., Kruszewski J., Ostachowicz W., Tarnowski J., Wittbrodt E.: The finite element metod in dynamics of structures (in Polish: Metoda elementów skończonych w dynamice konstrukcji), Arkady, Warszawa 1984.

[7] Adamiec-Wójcik I., Nowak A., Wojciech S.: Comparison of methods for modelling vibrations of collecting electrodes in dry electrostatic precipitators, Archive of Mechanical Engineering. Volume 60, Issue 3, pp. 431-449, ISSN (Print) 0004-0738, DOI: 10.2478/meceng-2013-0027

[8] Wittbrodt E., Adamiec-Wójcik I., Wojciech S.: Dynamics of flexible multibody systems rigid finite element method. Berlin Heidelberg New York: Springer, 2006.

[9] Adamiec-Wójcik I., Wojciech S.: The Rigid Finite Element Method in modelling vibrations of electrostatic precipitators (in Polish: Metoda sztywnych elementów skończonych w modelowaniu drgań elektrofiltrów), Modelowanie inżynierskie, 12(43), 2012, pp. 7-14.

[10] Abramowicz M.: Modelowanie drgań przestrzennych i identyfikacja parametrów dyskretnych modeli stalowo-betonowych belek zespolonych, PhD Thesis, West Pomeranian University of Technology Szczecin, 2014.

Modelowanie płyt i powłok z wykorzystaniem metody sztywnych elementów skończonych

S t r e s z c z e n i e

Metoda sztywnych elementów skończonych (SES) była dotychczas najczęściej stosowana do modelowania układów z podatnymi członami belkowymi (prętami). Przedmiotem niniejszej pracy jest modelowanie pojedynczego zestawu elektrod, składającego się z belki nośnej, zawieszonych na niej elektrod, będących powłokami o złożonym kształcie oraz drąga strzepującego. Do dyskretyzacji układu oraz elektrod zastosowano metodę sztywnych elementów skończonych. Wyniki obliczeń porównano z wynikami otrzymanymi przy zastosowaniu metody hybrydowej oraz pomiarów na specjalnym stanowisku badawczym.